Simulation of Supersonic Flow Over a Side Jet

Chung-Hao Wu[1], Yang-Yao Niu[1], Yi-Ju Chou[2]
[1]Department of Aerospace Engineering, Tamkang University, New Taipei City 25137, Taiwan
[2]Taida Institute of Mathematical Sciences, National Taiwan University, Taipei 10617, Taiwan

ABSTRACT

The following paper presents a numerical investigation of the interaction between supersonic crossflow and a side jet. The goal is to develop a two-dimensional numerical model that is capable of showing the detail physic phenomenon while a side jet injected into the flow field. A bow shock wave caused by the injection was formed and interacts with the separation shock wave and as the jet penetrates into the flow field, the jet is deflected and break up into a stream of small droplets.

1. Introduction

Multiphase flows cab be subdivided into four categories: gas-liquid, gas-solid, liquid-solid and three-phase flows. The first case, a liquid in a gas is as known as dispersed phase flow since one phase is dispersed and the other is continuous. Gas-solid flows are usually considered to be a gas with dispersed solid particle. Liquid-solid flows consist of flows in which solid particles are carried by the liquid and are referred to as slurry flow. In this article, liquid jet injection into crossflow is considered as the first case.

The study of liquid jet injection into a supersonic flow field has become an important research area as the development of high-speed flight vehicles. For high-performance of propulsion, the combustion efficiency depends strongly on the breakup, atomization, and evaporation of liquid fuel jet. Due to this purpose, developing a two-dimensional numerical model that is capable of showing the detail physic phenomenon especially on the jet break up, atomization is quite important.

In this study, we present a two-way coupling, Euler-Lagrangian model to simulate the crossflow field. We treat the side jet as Lagrangian particles and motion of the particles are described according to the Basset-Boussinesq-Oseen equation. To capture the motion, we use the concept of [1] particle-moving algorithm that moves particles by locally exchanging information between the Eulerian grid cell. The flow phase is evaluated by the Roe-type flux-difference splitting with a MUSCL spatial differencing scheme and using third-order of Runge-Kutta time-splitting method to reach better accuracy. The simulation performed by a Euler-Lagrangian model will show the detailed flow phenomena of a side jet injected into the flow field. The phenomenon including boundary layer separation, separation shock, bow shock,etc.

2. Mathematical Formulation

2.1 Equations of particle motion

The particle dynamics is described according to the Basset-Boussinesq-Oseen equation [1],” BBO-equation”. In this work, a spherical, small, non-deformable, non-rotating and non-collision particle is considered. The equation of motion illustrates the second law of Newton which mentions that the sum of forces acting upon a mass provides their acceleration. The particles trajectories are then deduced from the equation of motion.

$$\frac{du_p}{dt} = \underbrace{\frac{3}{4}\frac{C_D}{d}\frac{\rho}{\rho_p}\left(u-u_p\right)\left|u-u_p\right|}_{I} + \underbrace{\frac{1}{2}\frac{\rho}{\rho_p}C_{VM}\frac{d\left(u-u_p\right)}{dt}}_{II} + \underbrace{\frac{\rho}{\rho_p}\frac{\partial u}{\partial t}}_{III} + \underbrace{\left(1-\frac{\rho}{\rho_p}\right)g}_{IV} + \underbrace{\frac{9}{d_p}\frac{\rho}{\rho_p}\sqrt{\frac{\nu}{\pi}}C_B\int_{t_0}^{t}\frac{d(u-u_p)}{d\tau}\frac{1}{\sqrt{t-\tau}}d\tau}_{V} \quad (1)$$

Part I describes the drag force which is the drag force acts on the particle or droplet in a velocity field when there is no acceleration of the relative velocity between the particle and the fluid. Part II states the added mass force, when a body is accelerated through a fluid, there is a corresponding acceleration of the fluid which is at the expense of work done by the body. This additional work relates to the virtual mass effect, it can be neglected while droplets are small. Part III denotes the pressure gradient which applies a force on the particle and acts in the same direction as the pressure gradient itself. This force becomes important when the carrier gas density is higher compared to the density of the dispersed phase, which is not the case in this work, therefore it is neglected. Part IV states the buoyancy and gravitation forces. Part V denotes the Basset term. This term addresses the temporal delay in boundary layer development as the relative velocity changes with time, it's also neglectable while density ratio between fluid and droplets is small. The considered forces contributing to the motion of particle can be reduced as follow:

$$\frac{\partial u_p}{\partial t} = \frac{3}{4}\frac{C_D}{d_m}\frac{\rho}{\rho_p}\left(u-u_p\right)\left|u-u_p\right| + \left(1-\frac{\rho}{\rho_p}\right)g \quad (2)$$

where C_d stand for drag coefficient, d_m is diameter of droplets, u and u_p are the flow velocity and droplet velocity and g for gravity.

2.2 Compressible flows equations

The governing equation of motion used here for the two-dimensional the two-dimensional unsteady Navier-Stokes equations.

Corresponding author: Chung-Hao,Wu
E-mail address: wubug@hotmail.com

$$\frac{\partial \mathrm{Q}}{\partial \mathrm{t}}+\frac{\partial \mathrm{E}}{\partial \mathrm{x}}+\frac{\partial \mathrm{F}}{\partial y}=\frac{\partial E_v}{\partial \mathrm{x}}+\frac{\partial F_v}{\partial y}+S \tag{3}$$

and the Q flux vector for conservative variables, the E, F flux vector for inviscid terms, the E_v, F_v flux vector for viscous terms an S flux vector for the momentum transfer of the flow-particle interactions as shown in [2]

3. Numerical Methods

3.1 Numerical flux splitting

The inviscid fluxes of the Navier-Stokes equations are evaluated by the Roe-type flux-difference splitting with an MUSCL spatial differencing scheme. By splitting F into parts, where each part contains the information traveling in a particular direction, i.e., characteristic information, and the split fluxes are differenced according to the directions of the corresponding wave propagation, the interface numerical flux of each cell is expressed as

$$\hat{F}_{j+\frac{1}{2}}=\frac{1}{2}\left(F^R_{j+\frac{1}{2}}+F^L_{j+\frac{1}{2}}\right)-\frac{1}{2}(T|\Lambda|T^{-1})_{j+\frac{1}{2}}\delta Q_{j+\frac{1}{2}} \tag{4}$$

here $\delta\mathrm{Q}$ is the spatial difference $Q^R-\mathrm{Q}^L$. The fluxes $F^R=F(Q^R)$ and $F^L=F(Q^L)$ are computed using the reconstructed solution vectors Q^R and Q^L on the right- and left-hand sides of the cell face. Here Λ is the diagonal matrix of eigenvalues and T is the modal matrix that diagonalizes A where A is the viscous flux Jacobian, evaluated using a symmetric average between Q^R and Q^L.

3.2 Particle moving algorithm

The key element of this method is that in the computational framework, each grid cell possesses arrays that store the number of particles within that cell as well as the information of each particle.

At each time step, once the particle velocity is calculated from Eq. (2), by forth order Runge-Kutta time splitting method. According to the updated position, it is then determined whether the particle moves to the neighboring cells. If the particle moves to another cell, the associated particle information is deleted in the current cell, and the cell to which the particle moves adds an additional particle as well as the associated information. This is done by looping through each particle within a grid cell.

4. Results and Discussion

4.1 system description

The experiments were conducted under the inflow Mach number 1.5 configuration. The supersonic air flow entered into the domain in the direction parallel to the flat plate from the left side, and the liquid jet was injected from the wall. The inflow pressure was chose to be 1 atm and temperature at 25 ℃. The injector was located at 0.5 of the domain with a diameter 0.05 m. Computations grid are set as 144x51. Time step was chosen to be 2.e-4s in the current simulation. Particles are distributed uniformly along the width of the injector and injected 50 particles every 300 time steps.

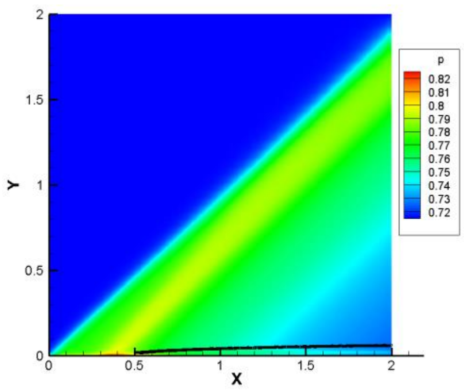

Fig. 1 Pressure contour (t = 7.5s, $\mathrm{d_p} = 50\mu\mathrm{m}$)

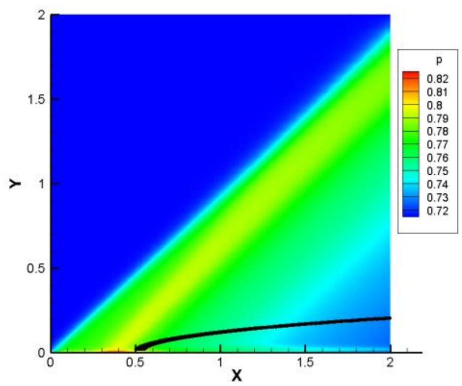

Fig. 2 Pressure contour (t = 7.5s, $\mathrm{d_p} = 200\mu\mathrm{m}$)

4.2 Conclusion

The result we can see here is that the trajectory goes higher with particle diameter. Momentum feedback is not enough to see the shock formation or boundary separation and other phenomenon. The phenomenon is not clear might due to too less particles, diameter too small or other reason.

References

[1] Y. J. Chou, S. H. Gu, Y. C. Shao, 2015, An Euler-Lagrange model for simulating fine particle suspension in liquid flows, Journal of Computational Physics, 299, 955-973.

[2] Y. Y. Niu, 2001, "Evaluation of Erosion in a Two-Way Coupled Fluid-Particle System," International journal for numerical methods in fluids, Vol. 36, pp. 711-742.